Fabrication of doubly-charged anion exchange membranes for enhancing hydroxide conductivity

Muhammad Imran Khan[1], Javier Fernandez-Garcia[2,*], Qi-Long Zhu[1,*]

[1]*State Key Laboratory of Structural Chemistry, Fujian Institute of Research on the Structure of Matter, Chinese Academy of Sciences, Fuzhou 350002, China*

[2]*School of Chemical and Process Engineering, University of Leeds, LS2 9JT, Leeds, UK*

J.FernandezGarcia@leeds.ac.uk; qlzhu@fjirsm.ac.cn

Abstract

Herein, a series of doubly-charged anion exchange membranes (AEMs) were fabricated by incorporating different amount of N-butyl substituted 1,4-diazabicyclo [2.2.2] octane (BDABCO) into brominated poly (2,6-dimethyl-1,4-phenylene oxide) (BPPO) via Menshutkin-reaction. The successful preparation of AEMs was confirmed by Fourier transform infrared (FTIR) spectroscopy. These AEMs were characterized physico-chemically in detail. These AEMs showed higher thermal, mechanical and chemical stability. The AEM with higher concentration of BDABCO exhibited hydroxide (OH^-) conductivity of 50.9 mS/cm and 84 mS/cm at 30 ºC and 80 ºC respectively. This demonstrated the as-prepared AEMs would be potential candidates for anion exchange membrane fuel cells.

Keywords: BPPO; Anion exchange membranes; Micro-phase separation; Alkaline stability; Hydroxide conductivity

1. Introduction

Presently, there are higher requirements in order to develop clean energy technology worldwide to solve the environmental issues due to pollution caused by

employing conventional fossil fuels [1]. Fuel cells are supposed to be environmentally positive energy generators that can extricate the potential energy stored in chemical fuels [2]. Among them, anion exchange membranes fuels cells (AEMFCs), promising option to proton exchange membrane fuel cells (PEMFCs), have got great attentions, because they combine the notable advantages including the much faster oxygen reduction kinetics operating under highly alkaline conditions and the permission of the usage of cheaper nonprecious metal catalysts (such as Ni, Fe and Co metals) [3, 4]. As one of the key components of AEMFCs, anion exchange membranes (AEMs) act as solid polymer electrolytes to conduct OH^- and separate the fuel from the oxidant [5]. However, the trade-off between electrochemical properties and mechanical/chemical stabilities in AEMs is more significant than that in proton exchange membranes (PEMs).

The meagre performance of AEMFCs is mainly associated to the lower conductivity of AEMs as compared with PEMs, such as Nafion [4]. The OH^- conductivity of AEMs is normally based on both the concentration and alkalinity of the functional groups and the efficient ion-conductive channels of the membrane matrix. The increased membrane hydroxide ion conductivity is related to the increased concentration of the function groups. However, higher ion exchange capacity (IEC) of AEMs is mostly inhibited because of their undue swelling. Meanwhile, highly alkaline functional groups, like guanidinium [6] and phosphonium [3, 7], are usually introduced into the membranes to further increase the OH^- conductivity. However, the enhancement of the conductivity of AEMs to the level of Nafion is not easy due to the innate disadvantages of OH^- conduction, which include (a) the lower mobility of OH^- compared with the proton (2.69 (OH^-) vs. 4.76 (H^+) relative to K^+ in infinitely dilute solution at 25 ^oC) and (b) the

insufficient dissociation and solvation of the hydroxide ion (pK_a~10, while for Nafion pK_a~ –6) [4, 8]. Therefore, it is especially crucial to design the organized hydroxide ion conductive channels within AEMs to enhance the hydroxide conductivity. Ion conductive channels in both AEMs and PEMs are thought to be generated because of the micro-phase separation of the hydrophilic ionic clusters from the hydrophobic polymer backbones [4]. Hydrophilic-hydrophobic micro-phase separation structures could effectively enhance the connectivity of ionic channels [9]. Therefore, AEMs with good micro-phase separation are excellent to get higher ionic conductivity. The higher OH^- conductivity can be attained at relatively low IEC by the AEMs with efficient hydroxide ion conductive channels, which in turn ease their mechanical and chemical stabilities. For instant, the ionic conductivity of poly(arylene ether sulfone) membrane (29 mS cm^{-1} at 20 °C) with the phase separation is higher than the one of the random copolymer (15 mS cm^{-1} at 20 °C) with the similar IECs [10]. Zhang *et al.* showed that the butyl substituted doubly-charged 1,4-diazabicyclo (2.2.2) octane (DABCO) including polymers exhibited better micro-phase separation as compared to the singly-charged analogues, and thereby gave the higher ionic conductivity [11].

The promotion of the micro-phase separation and the connectivity of efficient conductive channels in AEMs is still a challenging task due to the less hydrophobic non-fluorinated aromatic polymer backbones and inflexible quaternized groups knotted to the backbones [12]. Recently reported methodologies, such as incorporation of highly ionic blocks, [13-15] grafting with either hydrophilic or hydrophobic side chains [16-18] and introduction with inorganic fillers (such as imidazolium functionalized carbon nanotubes) [19], have provided effective ways to enhance the aggregation of ionic clusters into AEMs.

Nevertheless, the sophisticated synthetic procedures and the incompatibility of inorganic fillers with the polymer matrix restrict their widespread applications.

In the present research, we have reported the doubly-charged strategy to build efficient hydroxide ion conductive channels into the AEMs. By using the mono-cationic quaternary ammonium salt, namely N-butyl substituted 1,4-diazabicyclo [2.2.2] octane (BDABCO), a series of doubly-charged BPPO-based AEMs were developed by incorporating different concentrations of BDABCO into the polymer matrix. The structures of the as-prepared BDABCO-functionalized doubly-charged AEMs promote good micro-phase separation and efficient hydroxide ion conductive channels, as well as remarkable physico-chemical properties including water uptake (W_R), IEC, linear swelling ratio (LSR), mechanical strength, thermal and alkaline stability, thus affording the hydroxide conductivity as high as 50.9 and 83.7 mS cm^{-1} at 30 and 80 ^oC, respectively.

2. Experimental

2.1. Materials

Poly(2,6-dimethyl-1,4-phenylene oxide) (PPO) was purchased from Sigma Aldrich Co. Ltd. 1,4-diazabicyclo [2.2.2] octane (DABCO) and butyl bromide were Procured from Aladdin Industrial Corporation. 2,2′-Azo-bis-isobutyro nitrile (AIBN) and N-bromosuccinimide (NBS) were purchased from Adamas Reagent Co. Ltd. Chlorobenzene was bought from Shanghai Titas Co. Ltd. Sodium chloride (NaCl), sodium sulfate (Na_2SO_4), sodium hydroxide (NaOH), silver nitrate ($AgNO_3$), potassium chromate (K_2CrO_4), ethanol (EtOH), chloroform ($CHCl_3$), ethyl acetate (EtOAc) and 1-

methyl-2-pyrrolidone (NMP) were purchased from Sinopharm Chemical Reagent Co. Ltd. and were used as received. Deionized (DI) water was used through the work.

2.2. Preparation of brominated poly (2, 6-dimethyl-1,4-phenylene oxide) (BPPO)

BPPO was successfully synthesized according to the previously reported procedure [20]. In a typical method, 6 g of PPO (50 mmol) was dissolved into chlorobenzene (50 ml) in a round bottom flask containing a magnetic stirrer and reflexed condenser. N-bromosuccinimide (NBS) (4.45 g, 25 mmol), and 2,2'-azobis-isobutyronitrile (0.25 g, 1.5 mmol) were added into above stirred solution of PPO. The mixture was heated at 135 ºC for 3 hours. After chilling, the reaction mixture was poured into excess of ethanol to precipitate the product. The polymer was filtered and washed with ethanol, and the residue subsequently re-dissolved into chloroform (60 mL) and precipitated into excess of ethanol solution. The polymer was collected as a light-yellow powder and dried under vacuum for overnight to attain BPPO with a yield of 92 % and bromination ratio of 38 % (DB = 0.38).

2.3. Preparation of 1-butyl-4-aza-1-azaniabicyclo [2.2.2] octane bromide (BDABCO)

BDABCO was synthesized from DABCO and butyl bromide via a modified way as reported in the literature [11]. In a typical procedure, 10.00 g (0.089 mol) DABCO was dissolved in 100 mL of EtOAc at room temperature and then 14.68 g (1.2 times the molar amount of DABCO) butyl bromide was slowly added into the solution to stir it overnight. White crude suspension was separated by precipitation and washed by EtOAc many times. Finally, it was dried in vacuum oven at 60 °C. The preparation routes are represented in Scheme 1.

2.4. Preparation of doubly-charged AEMs

The preparation of doubly-charged BPPO-based AEMs was carried out by the solution-casting method as reported in our previous work [21-25]. In a typical procedure, 0.8 g of BPPO was dissolved into NMP to get homogeneous solution at room temperature. Then, different quantity of previously synthesized BDABCO was added into above solution. The reaction mixture was stirred at 40 ^{o}C overnight to complete the reaction between BPPO and BDABCO. After that, it was casted onto glass plate at 60 ^{o}C for 12 hours. Then, the transparent AEMs with two cyclic quaternary ammonium cations were obtained in bromide ionic form (Br^{-}). The attained membranes were denoted as PB-Br-x, where x is the percentage (25%, 38% and 50%) of BDABCO with respect to BPPO in the membrane matrices.

The membranes in OH^{-} form were obtained by immersing them into 1.0 M NaOH for 2 days at room temperature. Then, the resulting membranes were taken out from the NaOH, washed many times by DI water to completely remove the residual NaOH. The attained membranes were stored in water before using.

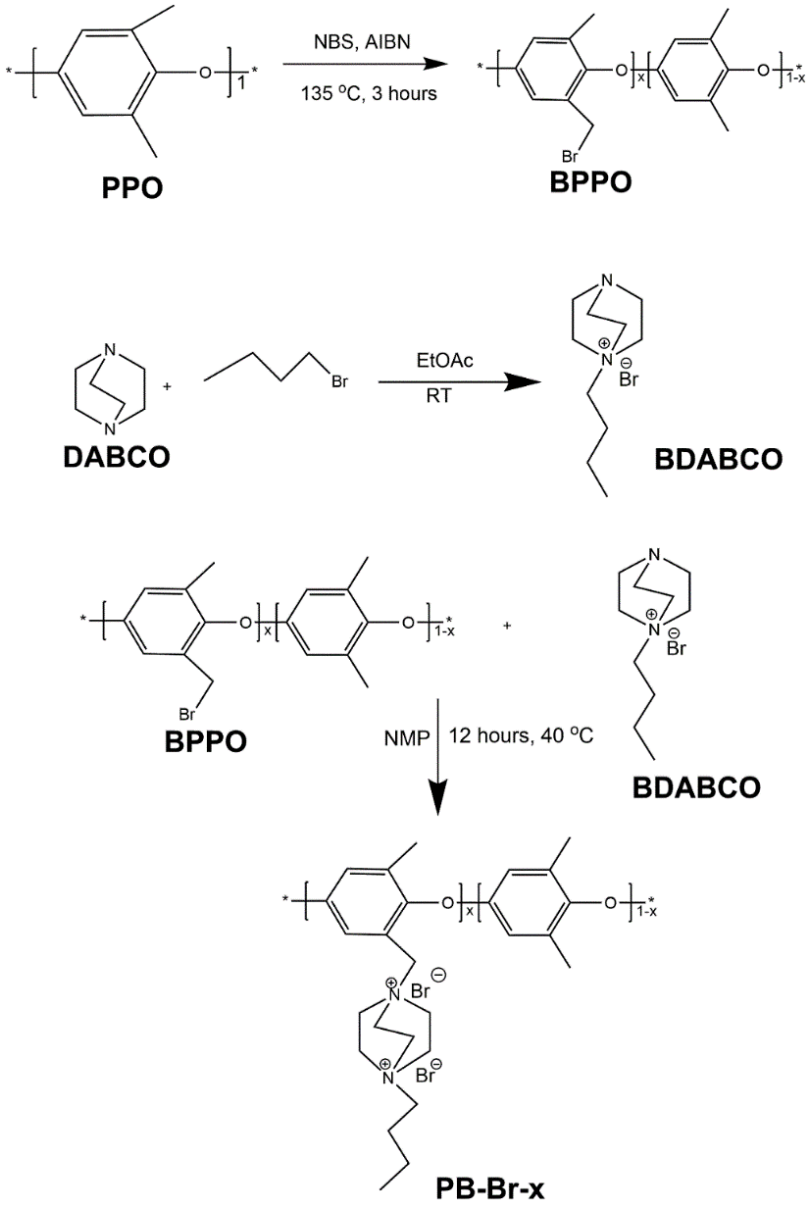

Scheme 1. Preparation of BPPO, BDABCO and anion exchange membranes.

2.5. Characterizations

2.5.1. Measurements

FTIR analysis of the prepared AEMs was carried out by employing FTIR spectrometer (Vector 22, Bruker) having resolution of 2 cm^{-1} and a total spectral range of

4000–400 cm^{-1}. DMX 300 NMR spectrometer operating at 300 MHZ was used in order to identify the chemical structures of the materials and products by ^{1}H NMR.

2.5.2. Ion exchange capacity (IEC)

IEC denotes the number of exchangeable ionic groups (equivalents) per dry membrane weight. Mohr method was used to calculate this [22, 26, 27]. The normal procedure for this is, firstly the prepared membrane samples were equilibrated in NaCl (1.0 M) solution for 48 hours such that all charge sites were changed into the Cl^- form. Then, the membranes were washed very cautiously with DI water to eliminate excess amount of NaCl. The washed membranes were then balanced with Na_2SO_4 (0.5 M) solutions for 48 hours. The amount of Cl^- ions liberated was calculated by titration with $AgNO_3$ (0.05 M) employing K_2CrO_4 as an indicator. The IEC (mmol g^{-1}) was measured by using following equation:

$$IEC = \frac{CV}{m} \tag{1}$$

where m, V and C denote the dry weight of the membrane, titre volume during titration and the concentration of $AgNO_3$ solution, respectively.

2.5.3. Water Uptake (W_R) and linear swelling ratio (LSR)

W_R is used to investigate the hydrophilicity of ion exchange membranes (IEMs). Membrane samples were dried in vacuum oven at 60 °C for 24 hours and accurately weighed to confirm their exact dry weight. Then, the membranes were submerged in DI water for 72 hours at room temperature and the wet weight of the membranes was measured after removal of surface water with tissue paper. Water uptake was measured from the difference in mass before and after complete drying the membranes as relative weight gain per gram of the dry sample using following equation [22, 26-28].

$$W_{\mathrm{R}} = \frac{W_{\mathrm{WET}} - W_{DRY}}{W_{DRY}} \times 100\% \quad (2)$$

where W_{WET} and W_{DRY} are the weights of wet and dry membranes, respectively.

LSR was measured by immersing the dry membranes (5.0 cm in length and 1.0 cm in width) into water for one day. It was measured by following equation:

$$LSR = \frac{L_{WET} - L_{DRY}}{L_{DRY}} \times 100\% \quad (3)$$

where L_{WET} and L_{DRY} are the lengths of wet and dry membranes, respectively.

2.5.4. Alkaline stability

The alkaline stability of the membranes was investigated by calculating the changes in IEC before and after being kept in 1.0 M NaOH at 60 ^{o}C for 30 days.

2.5.5. Mechanical and thermal stability

Q800 dynamic mechanical analyzer (DMA, TA Instruments) at a stretch rate of 0.5 N min^{-1} was used to determine the tensile strength of the hydrated. The samples were balanced in DI water for 24 hours and then cut into a rectangular shape with dimensions of 4.0 × 1.0 cm^2. A minimum of four specimens from each sample was considered. Shimadzu TGA-50H analyser within the temperature range of 25–800 ^{o}C under nitrogen flow, with a heating rate of 10 ^{o}C min^{-1} was used to determine the thermal stability of the membranes.

2.5.6. Microscopic Characterizations

A field emission scanning electron microscope (SEM, JSM-6700F) was used to investigate the morphology of the prepared membranes. Surface and cross-sectional images of membranes were considered from dry membranes. The SEM images of the

synthesized membranes were presented as representative cases. A veeco diInnova SPM, employing micro-fabricated cantilevers with a force constant of 20 Nm^{-1} was used to study the tapping-mode atomic force microscopy (AFM).

2.5.7. Hydroxide conductivity

The hydroxide conductivity of the prepared AEMs was measured by employing the four-point probe technique. An Autolab PGSTAT 30 (Eco Chemie, Netherland) in galvanostatic mode with AC current amplitude of 0.1 mA and a frequency range of 1 MHz–100 Hz was used to study the ionic conductivity. Bode plots were used to determine the frequency region, over which the magnitude of the impedance was constant; the ionic resistance was then determined from the associated Nyquist plot. The AEM under study was set into a Teflon cell where it was in touch with 2 current collecting electrodes and 2 potential sensing electrodes (the distance between the potential sensing electrodes was 1 cm). The cell was completely submerged into DI water and the impedance spectrum was determined. This was done as fast as possible to minimize the potential error caused by reaction of the hydroxide ions with dissolved carbon dioxide in the AEM, which could result in the formation of carbonate/bicarbonate anions and a reduced AAEM conductivity. The ionic conductivity was calculated according to the following equation:

$$\sigma = \frac{L}{Rwd} \tag{5}$$

where R is the membrane resistance, L is the distance between potential sensing electrodes, and W and d are the width and thickness of the membrane, respectively. At the pre-determined temperatures, the samples were equilibrated for a minimum of 30 min before the measurement.

3. Results and discussion

3.1. Preparation of BPPO and BDABCO

BPPO can be synthesized by simple bromination of commercially available poly (2,6-dimethyl-1,4-phenylene oxide) (PPO). It was carried out by employing AIBN as initiator and NBS as bromination agent. The structure of BPPO and its degree of bromination (DB) were investigated by ^{1}H NMR spectroscopy. Figure 1a depicts the ^{1}H NMR spectrum of prepared BPPO. It has been observed that the characteristic benzyl bromide group was present at 4.3 ppm. The DB was measured to be 38% from the integral area ratio between benzyl bromide group and unreacted benzyl signal at 2.1 ppm.

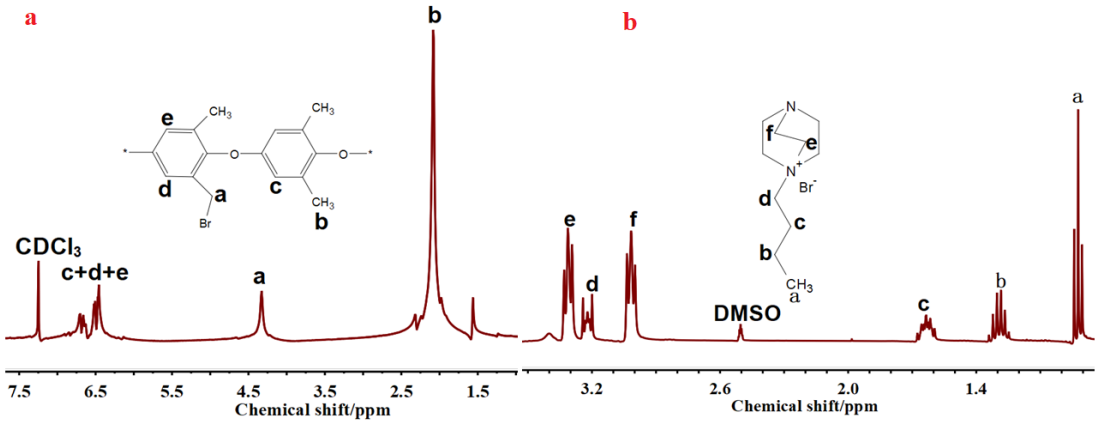

Figure 1 ^{1}H NMR spectra of (a) BPPO and (b) BDABCO.

BDABCO was prepared from N-butyl bromide and DABCO by a simple reaction (Scheme 1). The ^{1}H NMR spectrum of BDABCO (Figure 1 b) reveals the chemical structure and high purity of the prepared BDABCO, indicating that reaction performed as expected. The peak at 0.89 ppm is ascribed to $-CH_3$ whereas the peaks at 1.30, 1.50 and 3.20 ppm are associated to $-CH_2-$ of N-butyl bromide in BDABCO. The signals at 2.80 and 3.34 ppm are ascribed to $-CH_2-$ of cyclic ring.

3.2. FTIR analysis of membranes

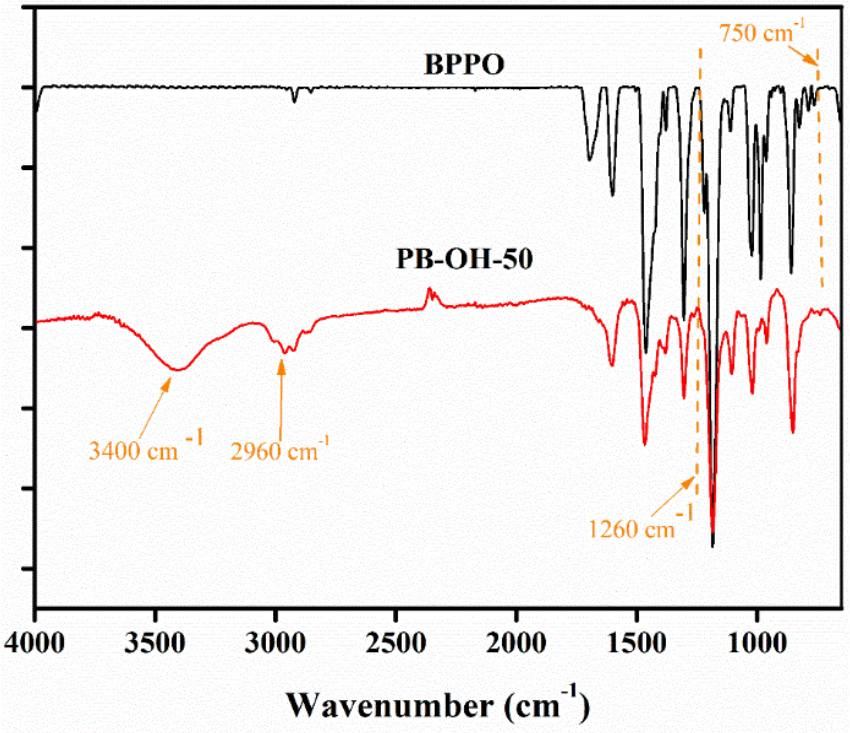

Figure 2 FTIR spectra of pristine BPPO and PB-OH-50 membranes.

The successful synthesis of BDABCO functionalized doubly-charged AEMs was confirmed by using FTIR spectroscopy. Taking PB-OH-50 membrane as an example, Figure 2 presents the FTIR spectra of pristine BPPO and PB-OH-50 membrane. By comparison, the spectrum of PB-OH-50 exhibited a new band at 1260 cm^{-1} which was absent in that of pristine BPPO. This is associated to the C–N stretching vibration representing the successful quaternization reaction. The band at 2960 cm^{-1} for $–CH_3$ stretching vibration was found to be increased in height and area due to the attachment of BDABCO containing methyl group after quaternization reaction. The broad band at 3400 cm^{-1} is associated to stretching vibration of –OH group in PB-OH-50. The characteristic band at 750 cm^{-1} is associated to the C–Br stretching in the pristine BPPO [21], which,

after the reaction with BDABCO, was disappeared. The results demonstrate the successful synthesis of BDABCO functionalized AEMs.

3.3. Ion exchange capacity

As a fundamental endowment, IEC exhibits a significant role in the water uptake, swelling ratio and hydroxide conductivity of AEMs, which provides information on the charge density, a significant parameter related to conductivity and transport properties of membranes [21]. The IEC of the doubly-charged AEMs was measured by classical Mohr's method and was given in Table 1. It was found to be increased from 1.64 mmol g^{-1} to 2.35 mmol g^{-1} with increasing the amount of BDABCO in the polymer matrix, namely an ascending order from membrane PB-OH-25 to PB-OH-50. The PB-OH-50 exhibited the highest IEC of 2.35 mmol g^{-1} among the prepared membranes. The introduction of BDABCO into polymer matrix provides double quaternary ammonium groups and therefore increases the hydrophilicity of the prepared doubly-charged AEMs.

Table 1 IEC, W_R, LSR and hydroxide conductivity of PB-OH-X membranes

Membranes	IEC (mmol g^{-1})	W_R (%)	LSR (%)	Conductivity[a] (mS cm^{-1})
PB-OH-25	1.64	11.76	2.78	11.4
PB-OH-38	2.05	13.33	2.94	35.5
PB-OH-50	2.35	25.49	3.24	50.9
QPPO	2.37	125	23.5	18.0 [29]

[a] Hydroxide conductivity was measured at 30 °C.

3.4. Water uptake and linear swelling ratio

For AEMs, water molecules are always significant in stimulating the dissociation of quaternary ammonium groups and transporting hydroxide ions. However, the thermal,

mechanical and dimensional stabilities of ion exchange membranes (IEMs) can be discriminated by larger volume fraction of water residing inside the membrane matrix [30, 31]. The AEMs require lower water uptake and reasonable hydroxide conductivity (at least 10 mS cm^{-1}) to use in fuel cell [31]. Therefore, the achievement of the balance of water uptake and hydroxide conductivity appears to be a big barrier in the preparation of high-performance AEMs [32]. Figure 3a depicts the water uptake of the prepared membranes in hydroxide ion (OH^-) form, which was enhanced with increasing the amount of BDABCO into the membrane matrix. It has been observed that PB-OH-25 exhibited a lower water uptake of 11.76% whereas PB-OH-50 exhibited a higher water uptake of 25.49% at room temperature, which should be due to the fact that PB-OH-50 has higher IEC and thus is more hydrophilic. The water uptake of the prepared membranes was also increased with increasing the temperature from 25-80 ºC, as presented in Figure 3a. The PB-OH-50 exhibited a water uptake of 88 % at 80 ºC, which is much lower than those of the previously reported BPPO-based AEMs [29]. Moreover, the water uptake of the prepared AEMs is found to be lower than the conventional QPPO membranes [33].

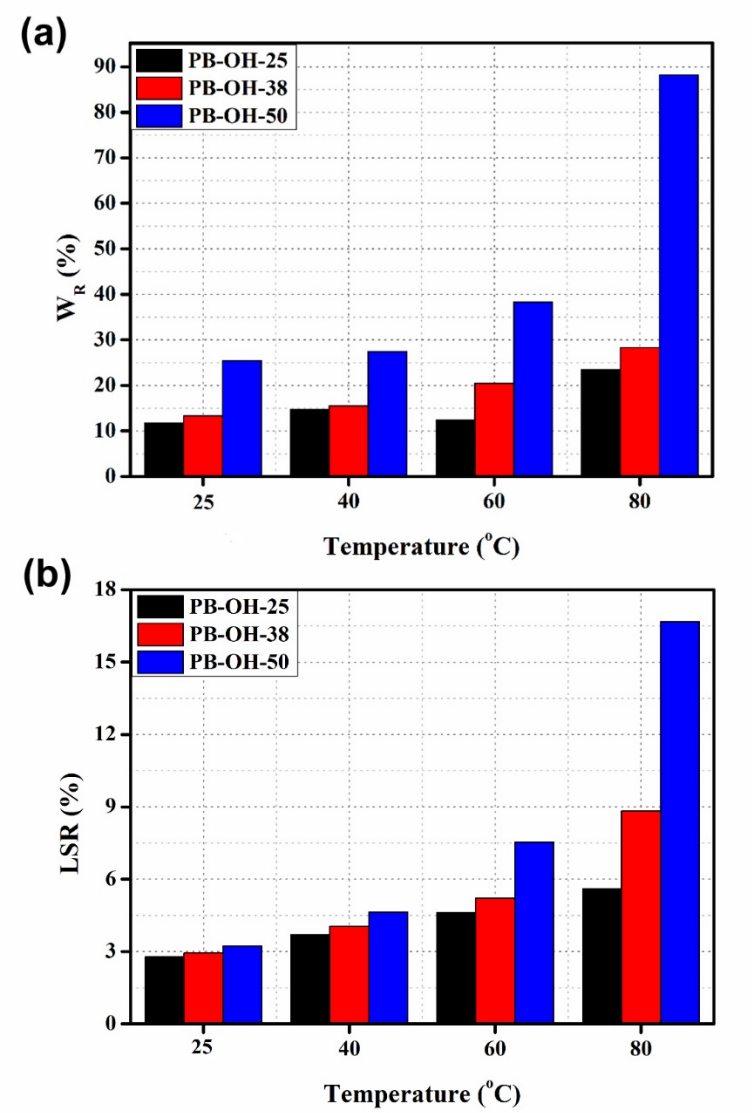

Figure 3 (a) Water uptakes and (b) linear swelling ratios of the prepared membranes at different temperatures.

The LSR of the prepared AEMs was measured at different temperatures and results are shown in Figure 3b. The LSR of the prepared membranes was found to be in the range of 2.78–3.24% at room temperature, which are much lower than those of the previously reported membranes [34]. The LSR at 25–80 °C was also investigated and found that PB-OH-50 with higher IEC exhibited LSR of 16.67 % at 80 °C. Thus, the developed AEMs with low LSR are capable of providing the higher dimensional stability

and therefore improving the hydroxide conductivity for AEMFC applications at elevated temperatures.

3.5. Thermal and mechanical stability

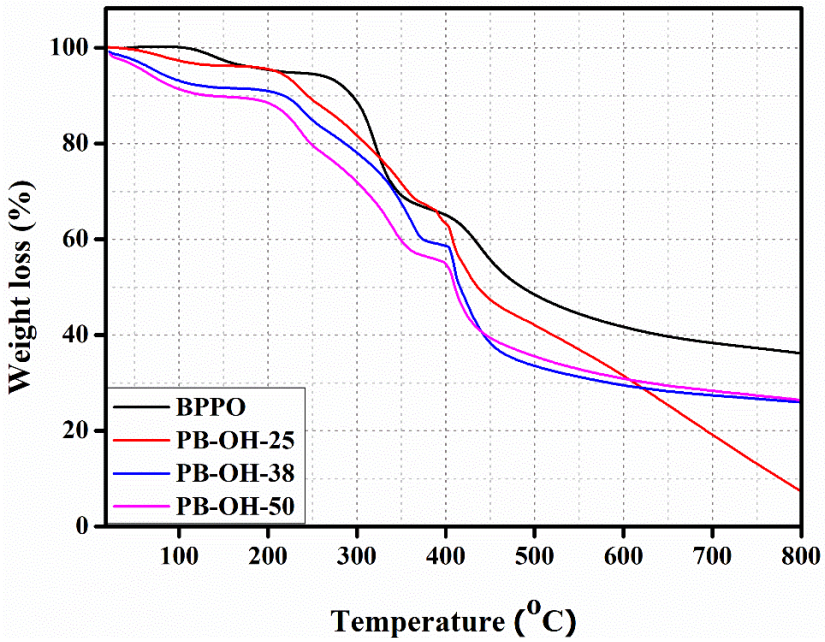

Figure 4 TGA thermograph of pristine BPPO membrane and the prepared AEMs.

Thermal stability of the prepared AEMs was investigated via thermogravimetric analysis (TGA) under nitrogen flow and the attained results are depicted in Figure 4. The obtained TGA thermograph showed that the weight loss of the prepared AEMs took place in three consecutive stages. The first weight loss stage underneath 130 °C is related to the evaporation of the adsorbed water and residual solvent. The second weight loss stage approximately at 240 °C is due to the degradation of the quaternary ammonium groups in the membrane matrix. The final weight loss stage around 440 °C is attributed to the decomposition of the polymer backbones. The obtained TGA results showed that the prepared doubly-charged membranes have good thermal stability and could be applied in AEMFCs.

The AEMs should exhibit sufficient mechanical stability for their applications in AEMFCs. The mechanical stability of the prepared doubly-charged AEMs was investigated in wet state via dynamic mechanical analysis (DMA) and the attained results are presented in Table 2. From PB-OH-25 to PB-OH-50 with increasing IEC, both the tensile strength (TS) and Young modulus decreased from 25.5 to 11.8 MPa and from 510.01 to 416.4 MPa, respectively, whereas the elongation at break (E_b) remained nearly unchanged (20.9–21.0%). This is a similar trend as reported in our previous research [21, 22]. It is associated to the increase in the hydrophilicity of the prepared membranes which results in their higher water uptake and swelling ratio. The water within AEMs can act as a plasticizer to crush the mechanical properties of membranes [35]; however, the prepared doubly-charged membranes PB-OH-X exhibited higher TS and lower E_b as compared to those reported previously [36], suggesting their excellent mechanical stability for applications in AEMFCs.

Table 2 Tensile strength, elongation at break and Young modulus of PB-OH-X membranes

Membranes	PB-OH-25	PB-OH-38	PB-OH-50
TS (MPa)	25.5±1.28	18.9±0.96	11.8±0.60
E_b (%)	20.9±1.05	20.9±1.05	21.0±1.10
Young modulus (MPa)	510.1±25.51	434.1±21.71	416.4±20.82

3.6. Morphology

The morphologies of the prepared membranes were studied in detail by scanning electron microscopy (SEM). Figure 5 depicts the SEM micrograph of surfaces and cross-sections of all prepared membranes from PB-OH-25 to PB-OH-50. The attained

micrograph showed that the surfaces and cross-sections of all prepared membranes are free from any pore, hole and crack, exhibiting their homogeneity and compactness, which is crucial for their application in AEMFCs. The homogeneity of the prepared AEMs is found to be enhanced with increasing the amount of ion exchange contents (BDABCO) into the membrane matrix.

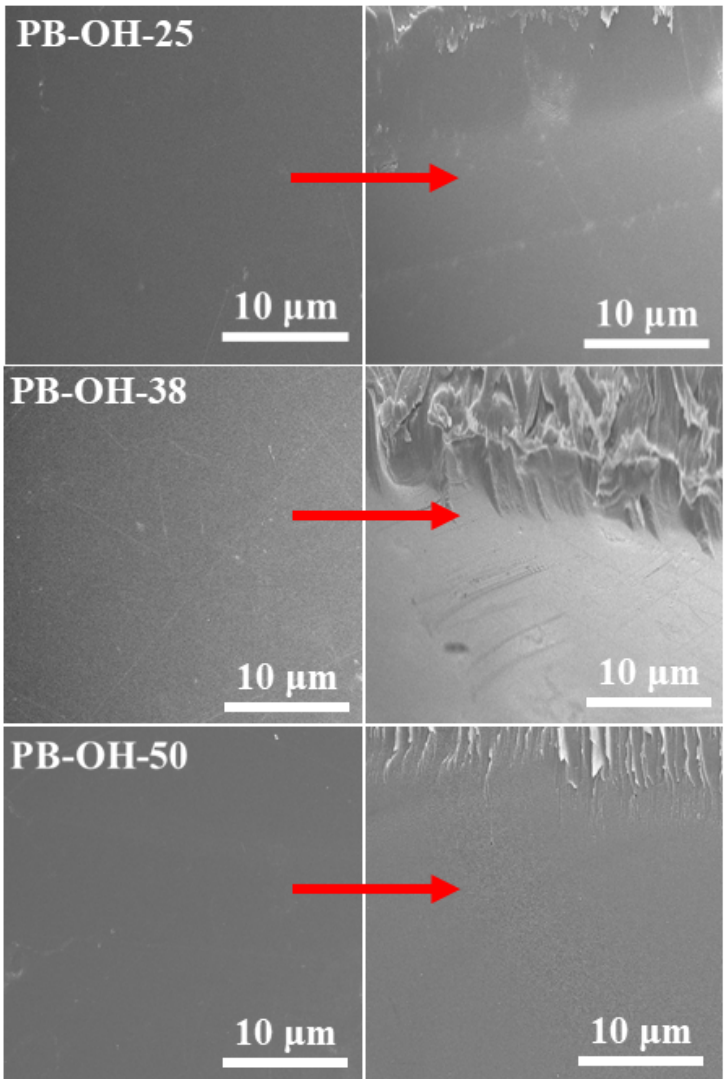

Figure 5 Surface (left) and cross-section (right) of the prepared AEMs.

The phase images of the prepared membranes PB-OH-X were recorded under ambient conditions by employing tapping-mode AFM and the results are shown in Figure

6. The darker areas denote the hydrophilic domains whereas brighter areas denote the hydrophobic domains [37]. The degree of phase separation and the size of ionic domains of all prepared membranes are clearly different, which is highly dependent on the concentration of ion exchange groups in the polymer matrix. As the concentration of BDABCO increases from PB-OH-25 to PB-OH-50, the more hydrophilic channels are produced due to the inter-connection of hydrophilic regions. These results provide an explanation of the rapid enhancement in water uptake and hydroxide conductivity of PB-OH-50.

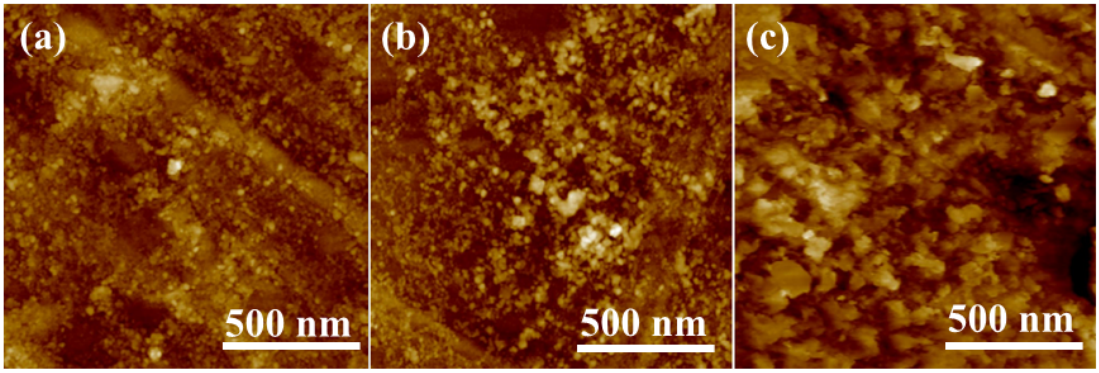

Figure 6 AFM tapping-phase images of (a) PB-OH-25 (b) PB-OH-38 and (c) PB-OH-50.

3.7. Chemical stability

The stability of the AEMs in alkaline medium is a highly referenced concern since they are employed in alkaline mediums. It is commonly known that the quaternary ammonium groups are quite unstable in alkaline condition, and the degradation involving direct nucleophilic displacement and Hofmann elimination, *etc.*, may occur [16]. The alkaline stability of the prepared doubly-charged membranes was studied by the changes in IEC upon alkaline treatment. For this, the prepared membranes were immersed in 1 M

NaOH solution at 60 ºC for one month (720 hours). The changes in IECs of the prepared AEMs after alkaline treatment are depicted in Figure 7. The IECs of the prepared membranes PB-OH-25, PB-OH-38 and PB-50 were found to be decreased to 49%, 43% and 42% of their initial values after 720 hours alkaline treatment at 60 ºC, which is due to the degradation of quaternary ammonium groups in the prepared membranes. The lower alkaline stability of the prepared AEMs is due the existence of several unprotected position [33]. It can be observed that the prepared AEMs possess several unprotected positions. Therefore, the hydroxide group (OH^-) can easily attach on these unprotected position which is responsible for fast degradation of quaternary ammonium group into the membrane matrix. As reported in previous research that the 1-methylimidazolium functionalized AEM possess less chemical stability than 1,2,4,5-tetramethylimidazolium functionalized AEMs because of presence of unprotected positions [33]. Moreover, it has already been reported in our research that the IEC of the conventional membrane QPPO was decreased to 55 % of its initial IEC only after 250 hours immersion in 1 M NaOH [21, 22]. It showed that the prepared doubly-charged AEMs exhibited better tolerance than QPPO under similar experimental conditions. This is associated to their steric hindrance of the N-butyl group bonded to the second quaternary ammonium group, as well as the better hydrophilic–hydrophobic micro-phase separated morphology as compared to QPPO.

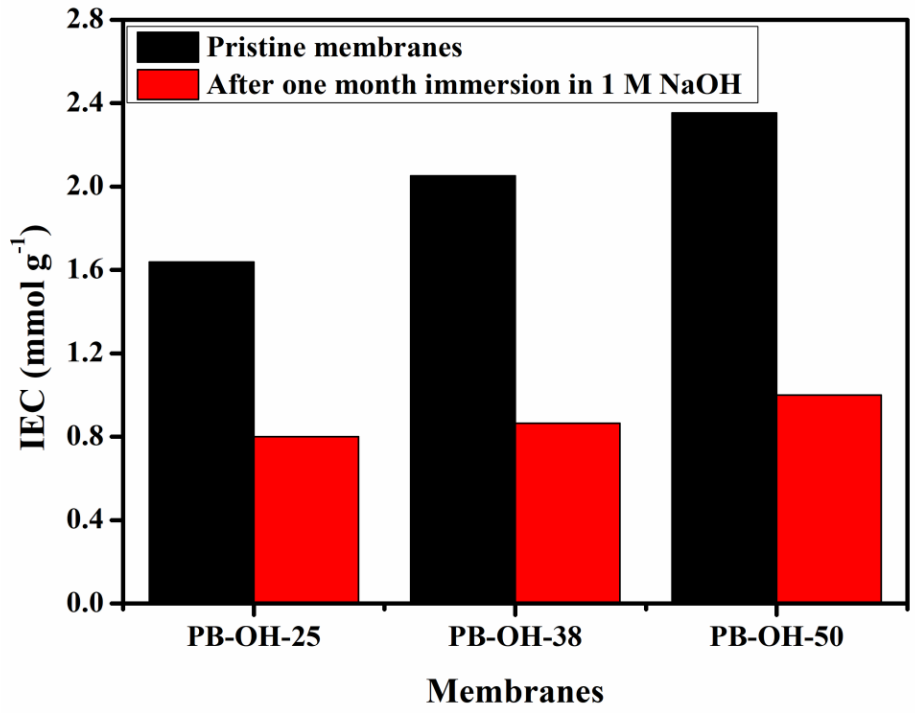

Figure 7 The changes in IEC of PB-OH-X membranes after immersion in 1 M NaOH for one month (720 hour).

3.8. Hydroxide conductivity and activation energy

The hydroxide conductivity is an important property of AEMs that plays a crucial role in the AEMFCs performance. The OH^- conductivity of an AEM is highly influenced by the ion exchange content in the polymer matrix. For AEMFC applications, there is a requirement for the OH^- conductivity to be higher than 10 mS cm^{-1} and for water uptake to be lower than 30% [38]. Therefore, the ionic conductivity of prepared doubly-charged AEMs was measured in deionized (DI) water with a four-point probe method at various temperatures. Figure 8a depicts the hydroxide conductivity of the investigated membranes as a function of temperature. It can be observed that the OH^- conductivity of all evaluated membranes is higher than 10 mS cm^{-1} at 30 ^oC which fulfills the

requirement of AEMFCs. Particularly noteworthy is that the PB-OH-50 (IEC = 2.35 mmol g^{-1}) exhibited highest ionic conductivity of 50.9 mS cm^{-1} at 30 ºC, which is much higher than that (18.0 mS cm^{-1}) of the conventional membrane QPPO (IEC = 2.37 mmol g^{-1}) [29]. The ionic conductivity of prepared doubly-charged membranes was found to be increased with increasing the concentration of BDABCO in membrane matrix because of the enhancement in their IECs, which is consistent with the rise in the concentration of active sites of anion (OH^-) transport and the volume fraction of water in the polymer matrix [39, 40]. Moreover, all the prepared membranes showed positive non-linear temperature conductivity correlations. The ionic conductivity of the prepared membranes was found to be increased with temperature because of the enhancement in the free volume and the accelerated mobility of hydroxide ion [38, 41]. The ionic conductivity of the prepared membranes PB-OH-25, PB-OH-38 and PB-OH-50 at 80 ºC reached to 20, 57 and 84 mS cm^{-1}, respectively. Table 3 depicts that the prepared doubly-charged membrane PB-OH-50 exhibited higher hydroxide conductivity than those of the previously reported AEMs at ambient temperatures. From the AFM tapping-phase images of PB-OH-50 (Figure 6), we can see that the hydrophilic domains (the dark areas) are uniformly dispersed throughout the entire membrane and hydrophilic channels are generated due to inter-connection of the hydrophilic regions which contain water for anion transport. Therefore, the high hydroxide conductivity of PB-OH-50 should be due to the reasons that BDABCO contains two chemically bound cations which exhibit stronger ionic interactions and better hydrophilic/hydrophobic micro-phase separation for facilitating OH^- transport. Hence, the BDABCO functionalized doubly-charged AEMs are more feasible for the enhancement of hydroxide conductivity.

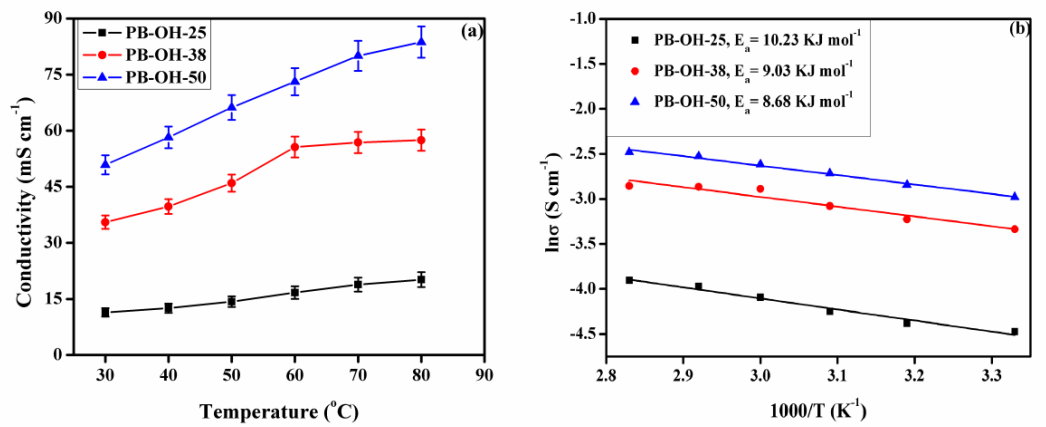

Figure 8 (a) Hydroxide conductivity as a function of temperature and (b) Arrhenius plot of 1000/T vs lnσ for the prepared AEMs.

The OH^- conductivity of the prepared doubly-charged AEMs was assumed to obey Arrhenius behavior.

$$\sigma = \sigma_o \exp(\frac{E_a}{RT}) \quad (6)$$

Where σ is the hydroxide conductivity σ_o is the pre-exponential factor and E_a is the activation energy. Therefore, the activation energy (E_a) of the prepared doubly-charged membranes for OH^- transportation was calculated by employing the regression line of 1000/T versus lnσ [42].

$$E_a = -b \times R \quad (7)$$

Where b is slope of fitting line and R is general gas constant (8.31 J K^{-1} mol^{-1}). The activation energy of the prepared doubly-charged membranes is presented in Figure 8b, which shows a reverse trend with the hydroxide conductivity of the prepared AEMs. The lower activation energy, as well as higher hydroxide conductivity, of PB-OH-50 indicates that more hydrophilic channels exist in this membrane. Therefore, it needs less energy for OH^- transfer compared with other AEMs.

Table 3 Comparison of hydroxide conductivity of the doubly-charged membrane PB-OH-50 with previously reported membranes

Membranes	Temperature (°C)	Hydroxide conductivity (mS cm^{-1})	References
PB-OH-50	30	50.90	This work
PBI-CPVBC/OH	25	25.7	[43]
M-BDIm-OH	20	16.1	[44]
0.5 QB-g-F0.2	30	44	[45]
Dim-PPO-0.54	30	40	[46]
PVA/C_4PIL	30	11.0	[47]
[Nbmd][OH]$_{40}$-QCS	30	5.80	[48]
AQPVBH-A	25	12.3	[49]
PES-B100-C16	30	18.9	[50]
NVC-50	20	19.84	[31]
PAES-Q-75	25	21.90	[51]
12-CQP-2	25	25.4	[52]
AD40i-OH	20	14.0	[53]
c-AEM-31	20	14.8	[54]
m-Am-PAEKS-3	20	26.0	[55]
sQPAE (1/4)-2	25	21.2	[56]
l-QPP-co-PAEK	30	11.0	[57]
C-QAPPESK/OH-5	25	10.4	[58]

4. Conclusions

In this article, we have successfully prepared BDABCO functionalized BPPO based doubly-charged AEMs via Menshutkin reaction. The prepared AEMs with homogeneous morphology exhibited high thermal, mechanical and chemical stability, which are crucial for AEMFC applications. The synthesized doubly-charged membranes exhibit lower water uptake and swelling ratio, which are benefit to their long-life use. The existence of BDABCO in the membranes matrix could expand ionic domain sizes and facilitate the generation of more interconnected ion-transport channels in the prepared

AEMs. Particularly, the prepared doubly-charged membrane PB-OH-50 (IEC = 2.35 mmol g^{-1}) exhibits high hydroxide conductivity of 50.9 mS cm^{-1} at 30 °C which is higher than that of the conventional membrane QPPO with similar IEC. These results show that the BDABCO functionalized BPPO based doubly-charged AEMs are promising candidates for potential applications in AEMFCs.

Acknowledgement

We thank the One Thousand Young Talents Program under the Recruitment Program of Global Experts, the National Natural Science Foundation of China (NSFC) (21901246, 21905278 and 21771179), and the Natural Science Foundation of Fujian Province (2019J05158 and 2019J01133) for financial support.

Conflicts of Interest

The authors declare no conflict of interest.

Reference

(1) Jacobson, M.Z.; Colella, W.G.; Golden, D.M. (2005) Cleaning the Air and Improving Health with Hydrogen Fuel-Cell Vehicles. *Science*, 308(5730): 1901-1905.

(2) Mauritz, K.A.; Moore, R.B. (2004) State of Understanding of Nafion. *Chem. Rev.* 104(10): 4535-4586.

(3) Gu, S.; Cai, R.; Luo, T.; Chen, Z.; Sun, M.; Liu, Y.; He, G.; Yan, Y. (2009) A Soluble and Highly Conductive Ionomer for High-Performance Hydroxide Exchange Membrane Fuel Cells. *Angew. Chem. Int. Ed.*, 48(35): 6499-6502.

(4) Merle, G.; Wessling, M.; Nijmeijer, K. (2011) Anion exchange membranes for alkaline fuel cells: A review. *J. Membr. Sci.* 377(1): 1-35.

(5) Wang, Y.-J.; Qiao, J.; Baker, R.; Zhang, J. (2013) Alkaline polymer electrolyte membranes for fuel cell applications. *Chem. Soc. Rev.* 42(13): 5768-5787.

(6) Zhao, C.H.; Gong, Y.; Liu, Q.L.; Zhang, Q.G.; Zhu, A.M. (2012) Self-crosslinked anion exchange membranes by bromination of benzylmethyl-containing poly(sulfone)s for direct methanol fuel cells. *Int. J. Hydrogen Energy*, 37(15): 11383-11393.

(7) Gu, S.; Cai, R.; Luo, T.; Jensen, K.; Contreras, C.; Yan, Y. (2010) Quaternary Phosphonium-Based Polymers as Hydroxide Exchange Membranes. *ChemSusChem*, 3(5): 555-558.

(8) Zhang, S.; Zhang, B.; Xing, D.; Jian, X. (2013) Poly(phthalazinone ether ketone ketone) anion exchange membranes with pyridinium as ion exchange groups for vanadium redox flow battery applications. *J. Mater. Chem. A*, 1(39): 12246-12254.

(9) Tsang, E.M.W.; Zhang, Z.; Shi, Z.; Soboleva, T.; Holdcroft, S. (2007) Considerations of Macromolecular Structure in the Design of Proton Conducting Polymer

Membranes: Graft versus Diblock Polyelectrolytes. *J. Am. Chemi. Soc.* 129(49): 15106-15107.

(10) Zhao, Z.; Wang, J.; Li, S.; Zhang, S. (2011) Synthesis of multi-block poly(arylene ether sulfone) copolymer membrane with pendant quaternary ammonium groups for alkaline fuel cell. *J. Power Sources*, 196(10): 4445-4450.

(11) Zhang, K.; Drummey, K.J.; Moon, N.G.; Chiang, W.D.; Long, T.E. (2016) Styrenic DABCO salt-containing monomers for the synthesis of novel charged polymers. *Polym. Chem.* 7(20): 3370-3374.

(12) Ran, J.; Wu, L.; Xu, T. (2013) Enhancement of hydroxide conduction by self-assembly in anion conductive comb-shaped copolymers. *Polym. Chem.* 4(17): 4612-4620.

(13) Rao, A.H.N.; Thankamony, R.L.; Kim, H.-J.; Nam, S.; Kim, T.-H. (2013) Imidazolium-functionalized poly(arylene ether sulfone) block copolymer as an anion exchange membrane for alkaline fuel cell. *Polymer*, 54(1): 111-119.

(14) Zhou, J.; Guo, J.; Chu, D.; Chen, R. (2012) Impacts of anion-exchange-membranes with various ionic exchange capacities on the performance of H2/O2 fuel cells. *J. Power Sources*, 219: 272-279.

(15) Kostalik, H.A.; Clark, T.J.; Robertson, N.J.; Mutolo, P.F.; Longo, J.M.; Abruña, H.D.; Coates, G.W. (2010) Solvent Processable Tetraalkylammonium-Functionalized Polyethylene for Use as an Alkaline Anion Exchange Membrane. *Macromolecules*, 43(17): 7147-7150.

(16) Li, N.; Leng, Y.; Hickner, M.A.; Wang, C.-Y. (2013) Highly Stable, Anion Conductive, Comb-Shaped Copolymers for Alkaline Fuel Cells. *J. Am. Chem. Soc.* 135(27): 10124-10133.

(17) Pan, J.; Chen, C.; Zhuang, L.; Lu, J. (2012) Designing Advanced Alkaline Polymer Electrolytes for Fuel Cell Applications. *Acc. Chem. Res.*, 45(3): 473-481.

(18) Zhang, Q.; Li, S.; Zhang, S. (2010) A novel guanidinium grafted poly(aryl ether sulfone) for high-performance hydroxide exchange membranes. *Chem. Commun.* 46(40): 7495-7497.

(19) Li, Q.; Liu, L.; Liang, S.; Dong, Q.; Jin, B.; Bai, R. (2013) Preparation and characterization of composite membranes with ionic liquid polymer-functionalized multiwalled carbon nanotubes for alkaline fuel cells. *RSC Adv.* 3(32): 13477-13485.

(20) Li, N.; Yan, T.; Li, Z.; Thurn-Albrecht, T.; Binder, W.H. (2012) Comb-shaped polymers to enhance hydroxide transport in anion exchange membranes. *Energy Environ. Sci.* 5(7): 7888-7892.

(21) Khan, M.I.; Zheng, C.; Mondal, A.N.; Hossain, M.M.; Wu, B.; Emmanuel, K.; Wu, L.; Xu, T. (2017) Preparation of anion exchange membranes from BPPO and dimethylethanolamine for electrodialysis. *Desalination*, 402: 10-18.

(22) Khan, M.I.; Mondal, A.N.; Tong, B.; Jiang, C.; Emmanuel, K.; Yang, Z.; Wu, L.; Xu, T. (2016) Development of BPPO-based anion exchange membranes for electrodialysis desalination applications. *Desalination*, 391: 61-68.

(23) Khan, M.I.; Luque, R.; Prinsen, P.; Rehman, A.; Anjum, S.; Nawaz, M.; Shaheen, A.; Zafar, S.; Mustaqeem, M. (2017) BPPO-Based Anion Exchange Membranes for Acid Recovery via Diffusion Dialysis. *Materials*, 10(3): 266.

(24) Khan, M.I.; Luque, R.; Akhtar, S.; Shaheen, A.; Mehmood, A.; Idress, S.; Buzdar, S.; Rehman, A. (2016) Design of Anion Exchange Membranes and Electrodialysis Studies for Water Desalination. *Materials*, 9(5): 365.

(25) Khan, M.I.; Khraisheh, M.; Almomani, F. (2019) Fabrication and characterization of pyridinium functionalized anion exchange membranes for acid recovery. *Sci. Total Environ.* 686: 90-96.

(26) Khan, M.I.; Mondal, A.N.; Cheng, C.; Pan, J.; Emmanuel, K.; Wu, L.; Xu, T. (2016) Porous BPPO-based membranes modified by aromatic amine for acid recovery. *Sep. Purif. Technol.* 157: 27-34.

(27) Khan, M.I.; Wu, L.; Hossain, M.M.; Pan, P.; Ran, J.; Mondal, A.N.; Xu, T. (2015) Preparation of diffusion dialysis membrane for acid recovery via a phase-inversion method. *Membr. Water Treat.* 6(5): 365-378.

(28) Khan, M.I.; Mondal, A.N.; Emmanuel, K.; Hossain, M.M.; Afsar, N.U.; Wu, L.; Xu, T. (2016) Preparation of pyrrolidinium-based anion-exchange membranes for acid recovery via diffusion dialysis. *Sep. Sci. Technol.* 51(11): 1881-1890.

(29) Ran, J.; Wu, L.; Varcoe, J.R.; Ong, A.L.; Poynton, S.D.; Xu, T. (2012) Development of imidazolium-type alkaline anion exchange membranes for fuel cell application. *J. Membr. Sci.* 415-416: 242-249.

(30) Chakrabarty, T.; Singh, A.K.; Shahi, V.K. (2012) Zwitterionic silica copolymer based crosslinked organic-inorganic hybrid polymer electrolyte membranes for fuel cell applications. *RSC Adv.* 2(5): 1949-1961.

(31) Mondal, A.N.; He, Y.; Ge, L.; Wu, L.; Emmanuel, K.; Hossain, M.M.; Xu, T. (2017) Preparation and characterization of click-driven N-vinylcarbazole-based anion exchange membranes with improved water uptake for fuel cells. *RSC Adv.* 7(47): 29794-29805.

(32) Pan, J.; Zhu, L.; Han, J.; Hickner, M.A. (2015) Mechanically Tough and Chemically Stable Anion Exchange Membranes from Rigid-Flexible Semi-Interpenetrating Networks. *Chem. Mater.* 27(19): 6689-6698.

(33) Zhu, Y.; He, Y.; Ge, X.; Liang, X.; Shehzad, M.A.; Hu, M.; Liu, Y.; Wu, L.; Xu, T. (2018) A benzyltetramethylimidazolium-based membrane with exceptional alkaline stability in fuel cells: role of its structure in alkaline stability. *J. Mater. Chem. A*, 6(2): 527-534.

(34) Guo, D.; Lai, A.N.; Lin, C.X.; Zhang, Q.G.; Zhu, A.M.; Liu, Q.L. (2016) Imidazolium-Functionalized Poly(arylene ether sulfone) Anion-Exchange Membranes Densely Grafted with Flexible Side Chains for Fuel Cells. *ACS Appl. Mater. Interfaces*, 8(38): 25279-25288.

(35) Dhakal, H.N.; Zhang, Z.Y.; Richardson, M.O.W. (2007) Effect of water absorption on the mechanical properties of hemp fibre reinforced unsaturated polyester composites. *Comp. Sci. Technol.* 67(7): 1674-1683.

(36) Tuan, C.M.; Kim, D. (2016) Anion-exchange membranes based on poly(arylene ether ketone) with pendant quaternary ammonium groups for alkaline fuel cell application. *J. Membr. Sci.* 511: 143-150.

(37) Wang, J.; Gu, S.; Xiong, R.; Zhang, B.; Xu, B.; Yan, Y. (2015) Structure–Property Relationships in Hydroxide-Exchange Membranes with Cation Strings and High Ion-Exchange Capacity. *ChemSusChem*, 8(24): 4229-4234.

(38) Wang, J.; Li, S.; Zhang, S. (2010) Novel Hydroxide-Conducting Polyelectrolyte Composed of an Poly(arylene ether sulfone) Containing Pendant Quaternary

Guanidinium Groups for Alkaline Fuel Cell Applications. *Macromolecules*, 43(8): 3890-3896.

(39) Siu, A.; Schmeisser, J.; Holdcroft, S. (2006) Effect of Water on the Low Temperature Conductivity of Polymer Electrolytes. *J. Phys. Chem. B*, 110(12): 6072-6080.

(40) Peckham, T.J.; Schmeisser, J.; Rodgers, M.; Holdcroft, S. (2007) Main-chain, statistically sulfonated proton exchange membranes: the relationships of acid concentration and proton mobility to water content and their effect upon proton conductivity. *J. Mater. Chem.* 17(30): 3255-3268.

(41) Lin, B.; Qiu, L.; Lu, J.; Yan, F. (2010) Cross-Linked Alkaline Ionic Liquid-Based Polymer Electrolytes for Alkaline Fuel Cell Applications. *Chem. Mater.* 22(24): 6718-6725.

(42) Slade, R.C.T.; Varcoe, J.R. (2005) Investigations of conductivity in FEP-based radiation-grafted alkaline anion-exchange membranes. *Solid State Ionics*, 176(5): 585-597.

(43) Lu, W.; Zhang, G.; Li, J.; Hao, J.; Wei, F.; Li, W.; Zhang, J.; Shao, Z.-G.; Yi, B. (2015) Polybenzimidazole-crosslinked poly(vinylbenzyl chloride) with quaternary 1,4-diazabicyclo (2.2.2) octane groups as high-performance anion exchange membrane for fuel cells. *J. Power Sources*, 296: 204-214.

(44) Hao, J.; Gao, X.; Jiang, Y.; Xie, F.; Shao, Z.; Yi, B. (2017) Fabrication of N1-butyl substituted 4,5-dimethyl-imidazole based crosslinked anion exchange membranes for fuel cells. *RSC Adv.* 7(83): 52812-52821.

(45) Ran, J.; Ding, L.; Yu, D.; Zhang, X.; Hu, M.; Wu, L.; Xu, T. (2018) A novel strategy to construct highly conductive and stabilized anionic channels by fluorocarbon grafted polymers. *J. Membr. Sci.* 549: 631-637.

(46) Lin, X.; Varcoe, J.R.; Poynton, S.D.; Liang, X.; Ong, A.L.; Ran, J.; Li, Y.; Xu, T. (2013) Alkaline polymer electrolytes containing pendant dimethylimidazolium groups for alkaline membrane fuel cells. *J. Materi. Chem. A*, 1(24): 7262-7269.

(47) Yang, Y.; Sun, N.; Sun, P.; Zheng, L. (2016) Effect of the bis-imidazolium-based poly(ionic liquid) on the microstructure and the properties of AAEMs based on polyvinyl alcohol. *RSC Adv.* 6(30): 25311-25318.

(48) Wang, D.; Wang, Y.; Wan, H.; Wang, J.; Wang, L. (2018) Synthesis of gemini basic ionic liquids and their application in anion exchange membranes. *RSC Adv.* 8(19): 10185-10196.

(49) Zhang, Y.; Fang, J.; Wu, Y.; Xu, H.; Chi, X.; Li, W.; Yang, Y.; Yan, G.; Zhuang, Y. (2012) Novel fluoropolymer anion exchange membranes for alkaline direct methanol fuel cells. *J. Colloid Interface Sci.* 381(1): 59-66.

(50) Lin, C.X.; Zhuo, Y.Z.; Lai, A.N.; Zhang, Q.G.; Zhu, A.M.; Liu, Q.L. (2016) Comb-shaped phenolphthalein-based poly(ether sulfone)s as anion exchange membranes for alkaline fuel cells. *RSC Adv.* 6(21): 17269-17279.

(51) Li, X.; Nie, G.; Tao, J.; Wu, W.; Wang, L.; Liao, S. (2014) Assessing the Influence of Side-Chain and Main-Chain Aromatic Benzyltrimethyl Ammonium on Anion Exchange Membranes. *ACS Appl. Mater. Interfaces*, 6(10): 7585-7595.

(52) Hossain, M.M.; Hou, J.; Wu, L.; Ge, Q.; Liang, X.; Mondal, A.N.; Xu, T. (2018) Anion exchange membranes with clusters of alkyl ammonium group for mitigating water swelling but not ionic conductivity. *J. Membr. Sci.* 550: 101-109.

(53) Kim, D.J.; Park, C.H.; Nam, S.Y. (2016) Characterization of a soluble poly(ether ether ketone) anion exchange membrane for fuel cell application. *Int. J. Hydrogen Energy*, 41(18): 7649-7658.

(54) Xue, J.; Liu, L.; Liao, J.; Shen, Y.; Li, N. (2017) UV-crosslinking of polystyrene anion exchange membranes by azidated macromolecular crosslinker for alkaline fuel cells. *J. Membr. Sci.* 535: 322-330.

(55) Xu, J.; Liu, B.; Luo, X.; Li, M.; Zang, H.; Zhang, H.; Wang, Z. (2017) Construction of ion transport channels by grafting flexible alkyl imidazolium chain into functional poly(arylene ether ketone sulfone) as anion exchange membranes. *Int. J. Hydrogen Energy*, 42(41): 25996-26006.

(56) Shi, Q.; Chen, P.; Zhang, X.; Weng, Q.; Chen, X.; An, Z. (2017) Synthesis and properties of poly(arylene ether sulfone) anion exchange membranes with pendant benzyl-quaternary ammonium groups. *Polymer*, 121: 137-148.

(57) Dong, X.; Xue, B.; Qian, H.; Zheng, J.; Li, S.; Zhang, S. (2017) Novel quaternary ammonium microblock poly (p-phenylene-co-aryl ether ketone)s as anion exchange membranes for alkaline fuel cells. *J. Power Sources*, 342: 605-615.

(58) Lu, W.; Shao, Z.-G.; Zhang, G.; Li, J.; Zhao, Y.; Yi, B. (2013) Preparation of anion exchange membranes by an efficient chloromethylation method and homogeneous quaternization/crosslinking strategy. *Solid State Ionics*, 245-246: 8-18.